JOURNAL OF MATERIALS SCIENCE: MATERIALS IN MEDICINE 5 (1994) 279–283

Structure and properties of hydroxyapatite-bioactive glass composites plasma sprayed on Ti6Al4V

J. H. CHERN LIN, M. L. LIU, C. P. JU
Department of Materials Engineering, National Cheng Kung University, Tainan, Taiwan

Hydroxyapatite (HA)-coated Ti6Al4V has recently been used as a bone substitute in orthopaedic and dental applications because of its favourable bioactivity and mechanical properties. Studies in the literature have shown that the bioactivity of calcium phosphate bioactive glass (BG) is higher than that of HA. In an attempt to increase the bioactivity of Ha-coated Ti6Al4V and enhance the bonding strength between coating and substrate, in the present study, HA/BG composites are applied onto Ti6Al4V using a plasma spraying technique. Microstructure and phase changes of the composite coatings after plasma spraying are studied. The coating–substrate bonding strength is evaluated using an Instron, following the ASTM C633 method. Results indicate that the average bonding strengths of BG, HA/BG and HA coatings are 33.0 $\pm$ 4.3, 39.1 $\pm$ 5.0, and 52.0 $\pm$ 11.7 MPa, respectively. Open pores with sizes up to 50 μm are found in both BG and HA/BG coatings, which are probably advantageous in including mechanical interlocking with the surrounding bone structure, once implanted. These HA/BG composites could provide a coating system with sufficient bonding strength, higher bioactivity, and a significant reduction in cost in raw materials. The future of this HA/BG composite coating system seems pretty bright.

1. Introduction

Hydroxyapatite(HA)-coated Ti6Al4V has been accepted as one of the most promising implant materials in orthopaedic and dental applications because of its favourable biocompatibility and mechanical properties [1–5]. Various coating techniques, such as dip coating-sintering, immersion coating, hot isostatic pressing (HIP), ion-plating and plasma spraying, have been used in coating HA on Ti or Ti–6Al–4V substrates [6–10]. Among these, plasma spraying appears to be the most favourable one in terms of mechanical properties, biocorrosion resistance, coating–substrate bonding strength, and process feasibility. Clinical studies of HA-coated total hip prosthesis and dental implants have shown satisfactory results [11–15], in which new bone formation was found on the surface of HA coating.

Nevertheless, due to the large difference in coefficient of thermal expansion (CTE) between HA ($13.3 \times 10^{-6}/°C$) and Ti6Al4V ($9.4 \times 10^{-6}/°C$) [16] and the high cooling rate involved in the plasma spraying technique, microcracks were frequently found within the coating as well as along the coating–substrate interface [17]. Some coating defects, such as cracking, flaking and scratching, were found in HA-coated implants which eventually led to delamination of the HA coating [18–20]. These delaminated HA particles were found in the surrounding bone tissue [19].

Concerning bioactivity, studies of calcium-phosphate bioceramics and a bioactive glass containing less than 60 wt % SiO_2 have shown that the bioactivity of calcium-phosphate bioactive glass was higher than that of pure HA [21]. When exposed to the body fluid, the bioactive glass underwent a biointegration process which involved biodissolution/biodegradation, apatite crystal precipitation, and the final bone formation onto the implant surface [21].

In an attempt to increase the bioactivity and, hopefully, at the same time maintain a bonding strength level of pure HA, in the present study, a series of HA/BG composite coatings have been plasma-sprayed onto a commercial Ti6Al4V substrate. Bonding strengths of these composite coatings were measured and compared with the existing pure HA bonding strength data in the literature. Phases and microstructure of the coatings were characterized by X-ray diffraction (XRD) and scanning electron microscopy (SEM).

2. Materials and methods

A commercial HA powder (Plasma Technik 6020) with particle size ranging from 44 μm to 125 μm was used in this study. This powder, specially prepared for plasma spraying in biomedical applications, is fabricated by Plasma Technik Company in Switzerland. The in-house fabricated bioactive glass contained frits

0957–4530

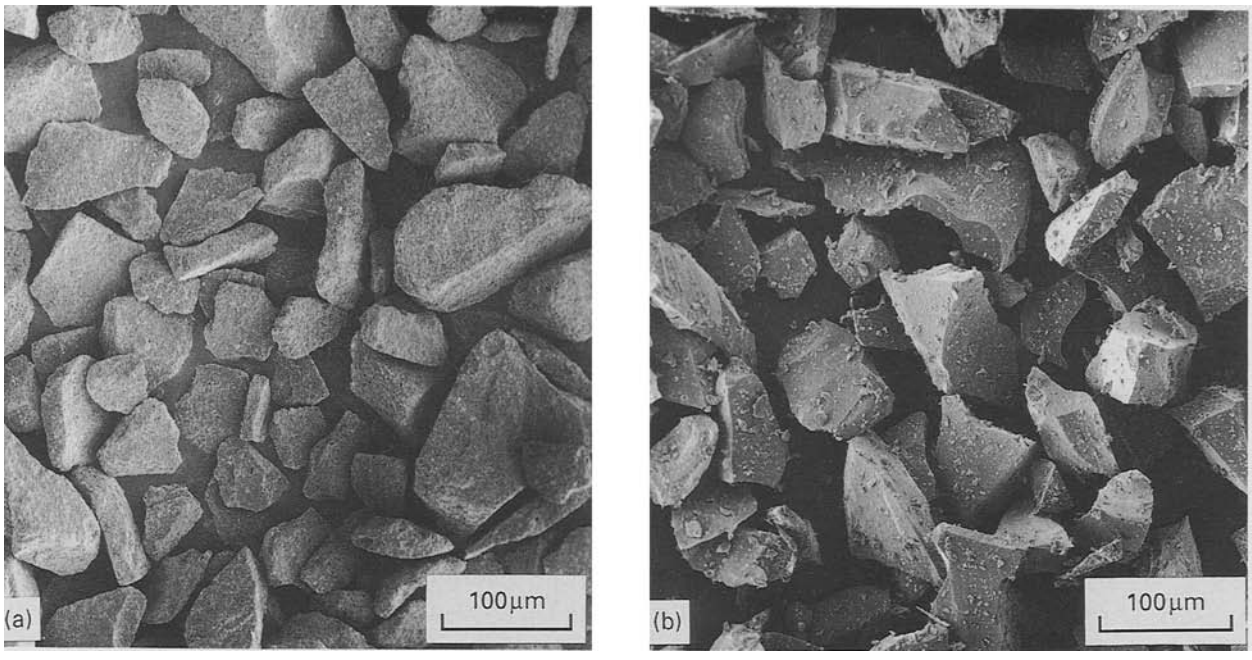

Figure 1 SEM micrographs of HA powder (a) and in-house fabricated bioglass powder (b).

of SiO_2, Na_2O, CaO and P_2O_5 with SiO_2 content less than 55 wt %. Appropriate amounts of the frits were mixed and melted at 1350 °C. After 2 h the melt was quenched in water and fractured fragments of the bioactive glass were obtained. These fragments were ball milled and sieved to obtain particles of size between 44 and 125 μm, which is comparable to the size of the HA powder. The HA and BG powders used for plasma spraying in this study are shown in Fig. 1. The irregular shape of the BG powder with sharp edges was a result of ball milling. Three kinds of coatings. i.e. pure HA, pure BG, and HA/BG composite (1:1 in powder weight), were produced.

Commercially available cylindrical rods and plates of Ti6Al4V were used as the substrate. Prior to plasma spraying, the substrate surfaces were mechanically polished through number 1200 grit, cleaned and sand-blasted. In order to obtain a uniform coating, the Ti6Al4V substrates were mounted on a disc which could rotate during spraying. A coating thickness of 150 μm was targeted throughout the study.

Phases of the coatings were analysed by XRD. A Rigaku D-max IIIV diffractometer operated at 30 kV and 20 mA was used. The surface morphology of the coatings was examined using an SEM (Hitachi S-2500). Specimens for cross-sectional microscopy were prepared by mounting the coated specimens in an epoxy resin, followed by polishing using 0.5 μm alumina.

The bonding strength testing method [22] for the flame-sprayed coatings suggested by ASTM C633-79, was used to measure the tensile bonding strength of the present coatings. To perform this test, two identical cylindrical Ti6Al4V rods, one with coating on a flat surface and the other without, were prepared. The flat surface of the uncoated rod, which was to be bonded to the coated rod, was roughened by sand blasting with 450 μm SiO_2 particles to enhance the resin adherence. A thin layer of bonding glue (Plasma Technik, Klebbi glue, Switzerland) was applied onto both coated and uncoated surfaces. The two rods were carefully aligned, using a special device as shown in Fig. 2. A compressive stress was applied to both rods during curing to ensure an intimate contact between resin and the two surfaces. After curing at 180 °C for 2–2.5 h in an oven, the bonded rods were bench cooled to room temperature, then the pressure was released and the resin-bonded rods were removed from the device. The coating–substrate bonding strength was measured using an Instron 8562 tester at a crosshead speed of 1.0 mm min^{-1}.

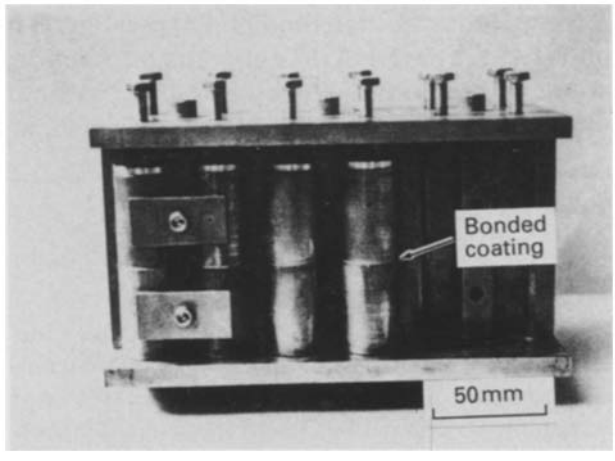

Figure 2 Bond-test fixture.

3. Results and discussion

The XRD patterns of raw HA powder, HA coating, BG coating and HA/BG composite coating are shown in Fig. 3. Due to the high temperature of the plasma, a surface layer of HA powder was melted and underwent phase transformation, as confirmed by XRD.

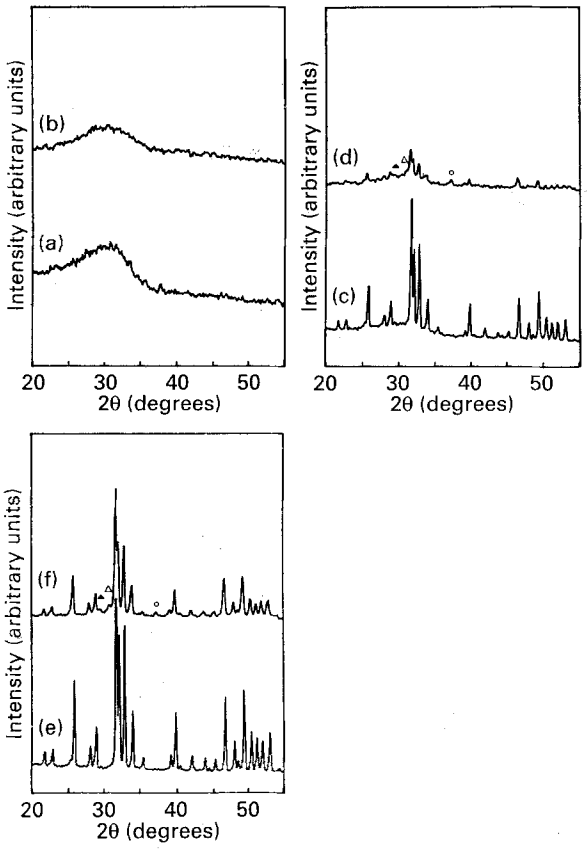

Figure 3 X-ray diffraction patterns of (a) BG powder; (b) BG coating; (c) HA/BG powder; (d) HA/BG coating; (e) HA powder; (f) HA coating (Δ: α-TCP, ○: CAO, ▲: $Ca_4P_2O_9$).

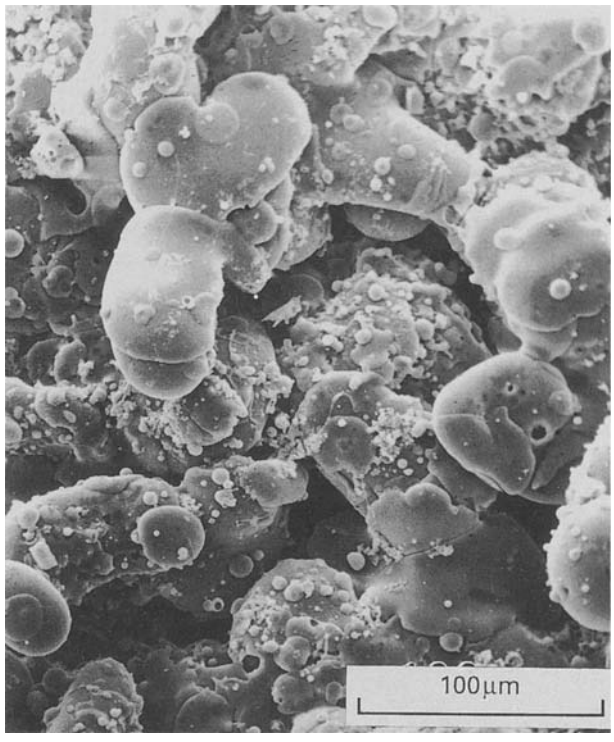

Figure 4 SEM micrograph of BG coated surface.

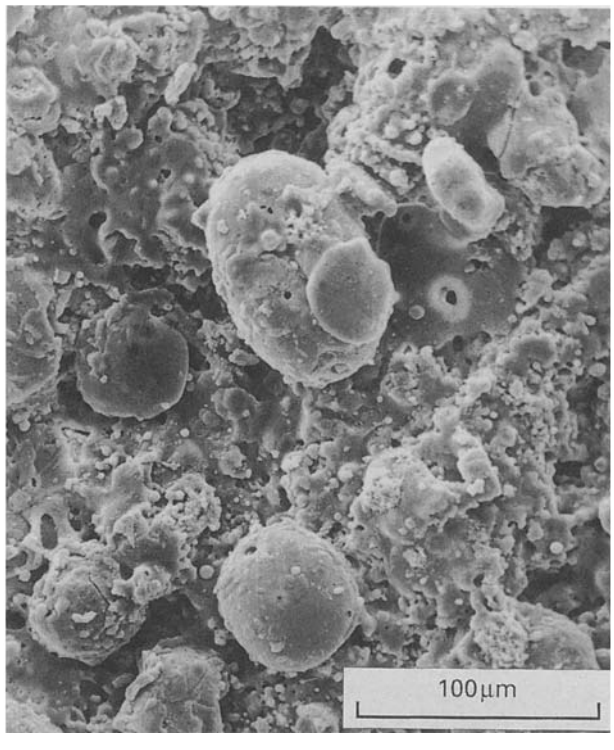

Figure 5 SEM micrograph of HA/BG composite coated surface.

Low intensity peaks of CaO, α-TCP and $Ca_4P_2O_9$ were found in both HA and HA/BG coatings. An essentially amorphous phase was identified in the BG coating. Since $Ca_4P_2O_9$, α-TCP and CaO are all biocompatible materials in a physiological environment, the existence of small amounts of these phases is not supposed to affect significantly biocompatibility of the coatings.

A secondary electron SEM micrograph of the BG-coated Ti6Al4V is shown in Fig. 4. Like other glasses, BG went through a softening state when heated. In this stage, the viscosity of BG became lower than that of the ceramic HA, which does not have a softening stage. Consequently, during plasma spraying the BG went through a low viscosity stage where bubbles were formed, probably due to the pressure exerted by the volatilized gases at high temperatures. These BG bubbles, some of which had been broken due to the high pressure internal gases, were solidified during cooling. Inside these broken bubbles some smaller globes were observed. A full explanation for this kind of structure is not yet established. Primarily due to the formation of these bubble-shaped particles, the surface roughness of the BG coating was the largest among the three coatings. Many pores with size up to 50 μm were found on the surface. These large surface pores, when implanted, might provide sites for bone ingrowth and therefore enhance the bonding between the implant and the surrounding bone structure.

An SEM micrograph of an HA/BG composite coating is shown in Fig. 5. In this coating, both bubble-shaped particles of BG and small irregular-shaped particles of HA were observed. The surface roughness of the HA/BG coating was lower than that of the pure BG coating but still much larger than the pure HA coating. Open pores with size up to 50 μm also existed on the surface. This indicates that, with the addition of BG in HA coating, large open pores

are formed due to the formation of the bubble-shaped BG particles on the composite coating surface. This might benefit, rather than degrade, the performance of HA/BG-coated implants by enhancing bonding between the coating and the surrounding bone structure. Also with the addition of BG in HA, the composite coating is expected to increase the bioactivity of the implants. As mentioned earlier, research has shown that the bioactivity of BG is higher than that of HA [20].

An SEM micrograph of a pure HA-coated surface is shown in Fig. 6. Quite different from the other two coatings, a smooth surface with evenly distributed small particles was observed in the HA coating. Obviously, in the absence of BG, the rough and porous surface feature no longer exists.

Cross-sectional SEM micrographs of the polished BG, HA/BG and HA coatings are shown in Figs 7, 8 and 9, respectively. A rough surface with large surface pores was again shown in the BG and HA/BG coatings. The appearance of the round holes was due to the sectioning of those bubble-shaped BG particles found in both BG and HA/BG coatings. These holes were distributed quite evenly throughout the coatings. In the HA-coated system, a denser and smoother coating was observed.

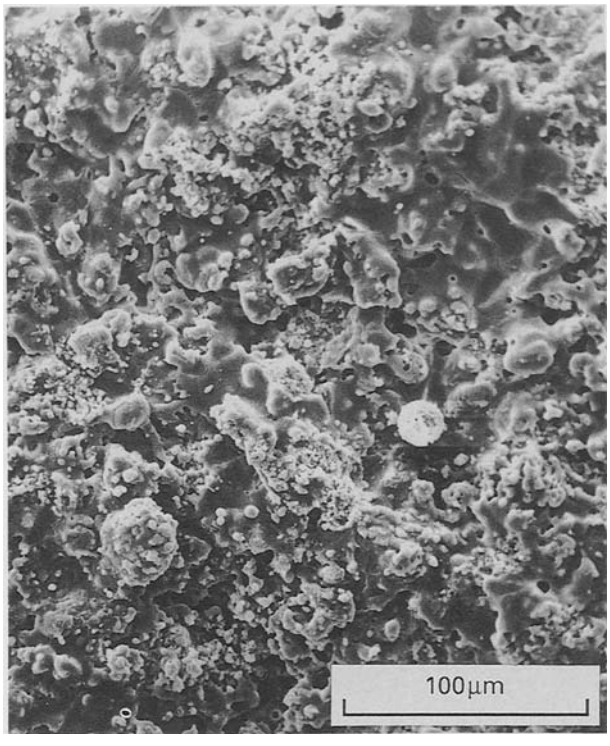

Figure 6 SEM micrograph of the HA-coated surface.

Using similar coating parameters, the coating thickness of HA was the largest ($\approx$ 150 μm) and that of BG was the smallest ($\approx$ 70 μm). The fact that the coating thickness decreased with BG content may be explained by the lower powder delivery rate of BG particles during plasma spraying. The sharp edges on the in-house fabricated BG particles may have caused this lower powder delivery rate.

Bonding strengths of the three systems were tested according to the method described earlier in Section 2. The post-testing observation showed that fractures of all systems occurred within the coating. Generally, only part of the coating was pulled out from the substrate, whereas the majority of the coating was still bonded tightly to the substrates. It was observed that the HA coating had the largest portion bonded, whereas the BG coating had the least. Since the "true" area of the coating pulled out from the substrate was hard to measure accurately, in this study, the original cross-sectional area of Ti6Al4V rods was used at all times in the calculation of bonding strength. The bonding strengths (average values of five to ten specimens) for BG, HA/BG and HA were determined to be 33.0 ± 4.3, 39.1 ± 5.0, and 52.0 ± 11.7 MPa, respectively. The highest measurable values for BG, HA/BG and HA were 39.0, 47.8 and 65.9 MPa, respectively. As discussed earlier, since extensive fracture occurred within the coatings themselves and the coatings were only partially pulled out from the surfaces of the substrates, the actual coating–substrate bonding strengths of BG, HA/BG and HA should be higher than the measured ones. Further, should the plasma spraying parameters for the BG and HA/BG coatings be improved, the bonding strengths of these two coatings are expected to increase further.

These HA/BG composites could provide a coating system with sufficient bonding strength, higher bioactivity, and a significant reduction in cost in raw materials. The future of this HA/BG composite coating system seems bright. Research on this composite system with other compositions is ongoing.

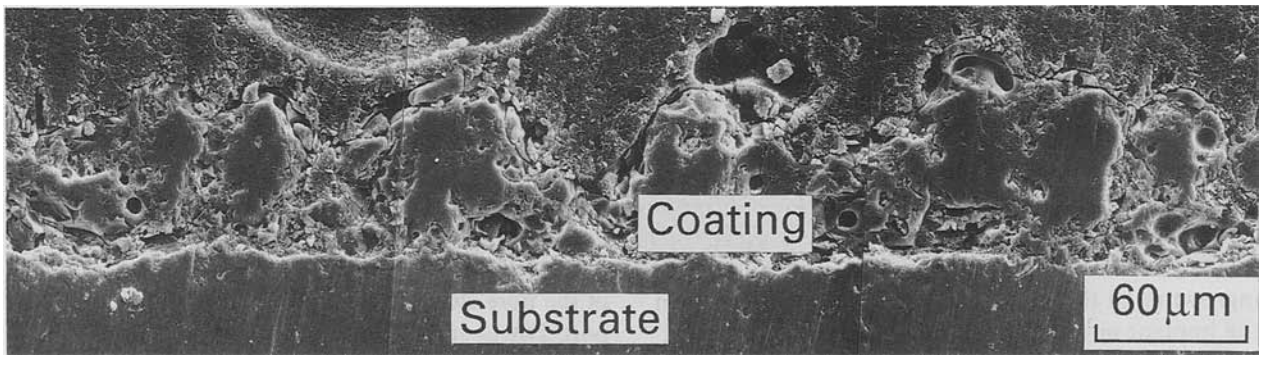

Figure 7 Cross-sectional SEM micrograph of BG coating.

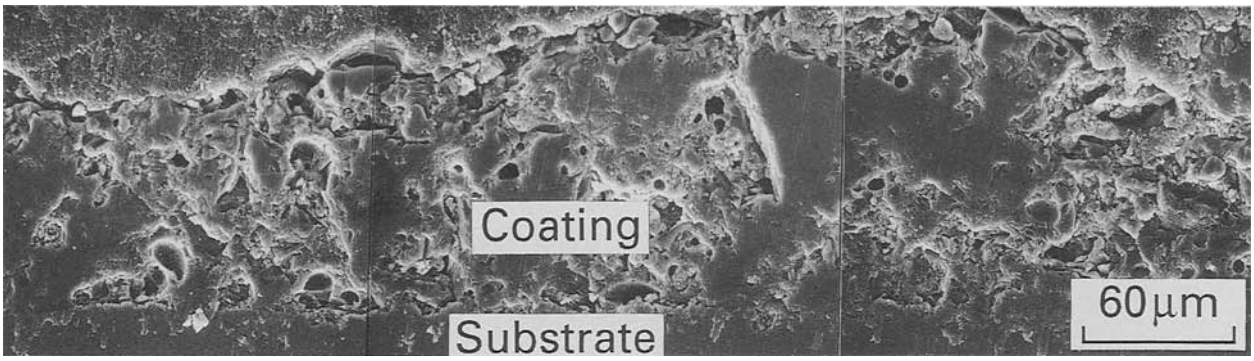

Figure 8 Cross-sectional SEM micrograph of HA/BG coating.

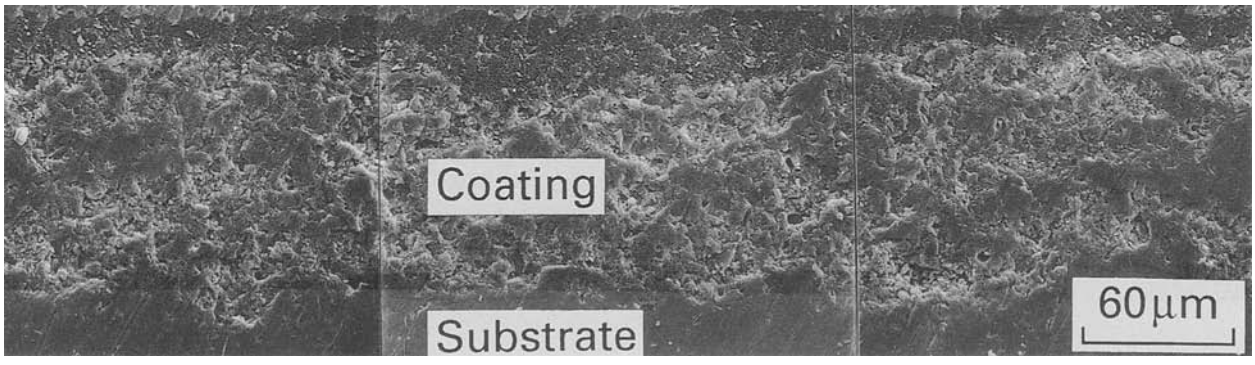

Figure 9 Cross-sectional SEM micrograph of HA coating.

4. Conclusions

Pure HA, pure BG and HA/BG composite coatings are plasma sprayed onto Ti6Al4V. Results indicate that the HA/BG composites could provide a coating system with sufficient bonding strength, and higher bioactivity and significant reduction in cost in new materials. This HA/BG composite coating system is promising and worth continued research.

Acknowledgements

The authors acknowledge with appreciation the support for this research by the National Science Council of Taiwan under contract number NSC 81-0405-E-006-32.

References

1. L. L. HENCH, R. J. SPLINTER, W. C. ALLEN and T. K. GREELEE, *J. Biomed. Mater. Res. Symp.* **2** (1971) 117.
2. T. KOKUBO, S. ITO, S. SAKKA and T. YAMAMURO, *J. Mater. Sci.* **20** (1985) 2001.
3. T. NAKAMURA, T. YAMAMURO, S. HIGASHI, T. KUKOBO and A. ITO, *J. Biomed. Mater. Res.* **19** (1985) 685.
4. R. G. T. GEESINK and K. DE. GROOT, *Clin. Orthop. Relat. Res.* **225** (1987) 147.
5. N. PASSUTI, G. DACULSI, J. M. ROGEZ, S. MARTIN and J. V. BAINVEL, *ibid.* **248** (1989) 69.
6. W. R. LACEFIELD, *Ann. NY Acad. Sci.* **523** (1988) 72.
7. C. S. KIM and P. DUCHEYNE, *Biomaterials* **12** (1991) 461.
8. M. YOSHINARI, K. OZEKI and T. SUMII, *Bull. Tokyo Dent. Coll.* **32** (1991) 147.
9. E. DORRE, *Biomed. Tech.* **34** (1989) 46.
10. K. DE GROOT, R. G. T. GEESINK, C. P. A. T. KLEIN and P. SEREKIAN, *J. Biomed. Mater. Res.* **21** (1987) 1357.
11. R. G. T. GEESINK, *Clin. Orthop. Relat. Res.* **261** (1990) 39.
12. J. A. D'ANTONIO, W. N. CAPELLO, O. D. CROTHERS, W. L. JAFFE and M. T. MANLEY, *J. Bone Joint Surg.* **74** (1992) 955.
13. S. D. COOK, J. ENIS, D. ARMSTRONG and E. LISECKI, *Dent. Clin. North Amer.* **36** (1992) 247.
14. J. N. KENT, M. S. BLOCK, I. M. FINGER, L. GUERRA, H. LARSEN and D. J. MISIEK, *J. Amer. Dent. Assoc.* **121** (1990) 138.
15. T. S. GOLEC and J. T. KRAUSER, *Dent. Clin. North Amer.* **36** (1992) 39.
16. S. MARUNO, K. HAYASHI, Y. SUMI, Y. F. WANG and H. IWATA, in "CRC handbook of bioactive ceramics", vol. II, edited by T. Yamamuro, L. L. Hench and J. Wilson (CRC Press, Boca Raton, 1991) p. 187–193.
17. S. D. COOK, K. A. THOMAS and J. F. KAY, *Clin. Orthop.* **265** (1991) 280.
18. H. W. DENISSEN, W. KALK, H. M. DE NIEUPORT, J. C. MALTHA, and A. VAN DE HOOFF, *Int. J. Prosth.* **3** (1990) 53.
19. T. W. BAUER, R. C. GEESINK, R. ZIMMERMAN and J. T. MCMAHON, *J. Bone Joint Surg.* **73** (1991) 1439.
20. J. LI, S. FORBERG and L. HERMANSSON, *Biomaterials* **12** (1991) 438.
21. L. L. HENCH, "Bioceramics: material characteristics versus in vivo behavior", edited by P. Ducheyne and J. E. Lemons (New York: New York Academy of Science, 1988) p. 54–71.
22. Annual book of ASTM standards, Vol. 15.02 (1984) 337.

Received 11 March
and accepted 25 November 1993